

## Optical absorption and luminescence investigations of the precipitated phases of $\text{Eu}^{2+}$ in NaCl and KCl single crystals

F. J. López,\* H. Murrieta S., J. Hernández A., and J. Rubio O.

*Instituto de Física, UNAM, P.O. Box 20-364, México 20, D.F., México*

(Received 1 May 1980)

A detailed study of the optical absorption and luminescence spectra associated with the precipitated phases of divalent europium in NaCl and KCl single crystals is reported. For the system NaCl-EuCl<sub>2</sub>, three fluorescence bands peaking at 410, 439, and 485 nm were observed in crystals which were stored for six years at room temperature, without any previous heat treatment. The corresponding optical-absorption spectrum of these crystals consists of two broad bands peaking at 260 and 349 nm with a cubic crystalline field splitting  $10Dq = 9809 \text{ cm}^{-1}$ . After quenching the crystals from 600 °C, only one emission band peaking at 427 nm was observed and the corresponding optical-absorption spectrum consists also of two broad bands but now peaking at 240 and 347 nm with a  $10Dq$  splitting of  $12849 \text{ cm}^{-1}$ . The emission band at 410 nm in the well-aged crystals was associated with the stable dihalide phase EuCl<sub>2</sub>, while those peaking at 439 and 485 nm were ascribed to the metastable precipitated EuCl<sub>2</sub>-like plate zones parallel to  $\{111\}$  and  $\{310\}$  planes of the matrix lattice, respectively. For the system KCl-EuCl<sub>2</sub>, only one emission band peaking at 427 nm was observed in crystals stored at room temperature for five years, without any previous heat treatment. The corresponding optical-absorption spectrum of these well-aged crystals consists of two broad bands peaking at 244 and 349 nm with a  $10Dq$  value of  $12331 \text{ cm}^{-1}$ . After quenching the samples, an emission band at 419 nm was observed and the corresponding optical-absorption spectrum was very similar to that observed before the quenching, although its  $10Dq$  splitting was smaller ( $11997 \text{ cm}^{-1}$ ). In this case, the band peaking at 427 nm, observed in the well-aged crystals, has been tentatively associated with the metastable Suzuki phase of divalent europium in the potassium chloride host. The change in the absorption, excitation, and emission spectra associated with the different precipitated phases of  $\text{Eu}^{2+}$  in NaCl and KCl as a function of the annealing temperature is also reported.

### I. INTRODUCTION

Precipitation of a phase containing divalent ions from an alkali halide solid solution can take different structural forms. Suzuki<sup>1-5</sup> has performed an extensive study by x-ray diffraction of the nature of the precipitates in the alkali halides. According to this author, in the system NaCl-CdCl<sub>2</sub> the ions segregate on the  $\{100\}$  planes to form platelets of a metastable phase with the stoichiometry  $6\text{NaCl} \cdot \text{CdCl}_2$ . This metastable phase is essentially an ordered arrangement, on the NaCl lattice, of the  $\text{Na}^+$  and  $\text{Cd}^{2+}$  ions, cation vacancies, and  $\text{Cl}^-$  ions, the latter retaining their original sites but being displaced slightly toward the divalent cadmium ion. It is known that this kind of preprecipitate is also produced in the systems NaCl-MgCl<sub>2</sub>,<sup>6</sup> NaCl-NiCl<sub>2</sub>,<sup>7</sup> NaCl-FeCl<sub>2</sub>,<sup>8</sup> and NaCl-MnCl<sub>2</sub>,<sup>9</sup> although it does not form in NaCl-CaCl<sub>2</sub> (Ref. 4) after a whole variety of heat treatments. For the latter system, Suzuki<sup>4</sup> found characteristic reflections of x rays corresponding to a rodlike distribution. These diffuse reflections were interpreted as being due to precipitation of small platelike structures,

called the plate zones, parallel to  $\{111\}$  and  $\{310\}$  planes of the matrix lattice. The plate zones were considered to be composed of a number of smaller units, called platelets, which are disposed in antiphase relation among themselves in a plate zone. When the crystals were kept for 3 days at room temperature after quenching, precipitates were composed of  $\{310\}$  plate zones only, and the  $\{111\}$  plate zones scarcely appeared after a month. At a later stage of precipitation, CaCl<sub>2</sub> crystallites appeared in the matrix. When the crystals were heated at 100 °C and then quenched, both kinds of platelets were observed. As the temperature was increased, the  $\{111\}$  platelets gave rise to more intense diffuse spots in the diffraction pattern while those due to the  $\{310\}$  platelets nearly disappeared. At the same time reflections were observed due to the stable dihalide phase CaCl<sub>2</sub>, which is incoherent with the matrix, and which grew up from the  $\{111\}$  plate zones. This latter kind of precipitate has been reported to nucleate in the systems NaCl-SrCl<sub>2</sub>,<sup>10</sup> NaCl-EuCl<sub>2</sub>,<sup>11</sup> and NaCl-BaCl<sub>2</sub>.<sup>12</sup> The structures of the  $\{111\}$  and  $\{310\}$  platelets were proposed by Suzuki to be two-dimensionally periodic

along directions parallel to the plane of the platelet, with a stoichiometry similar to that of  $\text{CaCl}_2$ , although retaining coherency with the matrix.

Recently, two of the present authors (J.H.A. and J.R.O.) have performed an investigation dealing with the thermal resolution of the stable segregated phase  $\text{EuCl}_2$  of the divalent europium ion in monocrystalline sodium chloride<sup>11</sup> using optical absorption and electron paramagnetic resonance (EPR) techniques. It was found that the dissolution of the segregated phase, which results in the growth of  $\text{Eu}^{2+}$ -cation vacancy dipoles, takes place in the range 227–450 °C.

In the present paper we report a detailed study of the optical absorption and luminescence spectra associated with the different precipitated phases of  $\text{Eu}^{2+}$  in NaCl and KCl single crystals. It is shown that both the optical absorption and the luminescence spectra depend strongly on the kind of precipitate which has been nucleated in the matrix. For the system NaCl- $\text{EuCl}_2$ , in addition to the stable dihalide phase  $\text{EuCl}_2$ , two metastable phases were also observed. They have been ascribed to the precipitated plate zones extending parallel to  $\{111\}$  and  $\{310\}$  planes of the matrix lattice with a stoichiometry similar to  $\text{EuCl}_2$  but maintaining coherency with the matrix. On the other hand, for the system KCl- $\text{EuCl}_2$  only one precipitated phase was observed and it has been tentatively associated with the metastable Suzuki phase of  $\text{Eu}^{2+}$  in this lattice. The change in the absorption, excitation, and emission spectra associated with the different precipitated phases of divalent europium ions in NaCl and KCl as a function of the thermal treatment is also reported.

## II. EXPERIMENTAL

Single crystals of sodium and potassium chloride doped with divalent europium were grown in our laboratory using the Czochralski method under a controlled atmosphere (dry argon) in order to minimize contamination by OH,  $\text{H}_2\text{O}$ , and oxygen which are present in air and could affect the solubility and precipitation phenomena. Doping was achieved by adding to the melt different initial concentrations of  $\text{EuCl}_2$ , which was previously reduced from  $\text{EuCl}_3 \cdot 6\text{H}_2\text{O}$  using standard techniques.<sup>13</sup> The concentration of the impurity in the samples was determined directly from the optical-absorption spectrum using our previously determined calibration constants between the optical-absorption coefficient of the high-energy band and the number of divalent europium ions expressed in ppm.<sup>14</sup> In a few experiments, crystals of NaCl and KCl doped with  $\text{Eu}^{2+}$ , kindly supplied by J. J. Martin from Oklahoma State University have also been utilized, results being essentially similar in all cases. Thermal quenching was performed by heating the samples to the desired

temperature and then dropping them onto a copper block at room temperature (25 °C). The highest temperature used was 600 °C. Annealing treatments were carried out in a standard furnace with temperature control in the range  $\pm 3$  °C.

Optical-absorption measurements were made at room temperature with a Perkin-Elmer model 330 double-beam recording spectrophotometer with capability to record up to the fourth-order derivative of the absorption spectrum. Luminescence measurements were also performed at room temperature with a Perkin-Elmer model 650-10 S fluorescence spectrophotometer using a 150-W xenon lamp; the resolution being 2 nm or better in all cases. To measure the decay of europium-cation vacancy dipoles as a function of the time elapsed after quenching, a Varian EPR model E-104 spectrometer operating at X-band frequencies was employed.

## III. RESULTS

### A. Optical absorption

#### 1. NaCl samples

The  $\text{Eu}^{2+}$  ion in the alkali halides produces two broad bands in the ultraviolet region of the absorption spectrum, which are due to transitions from the  $4f^7$  ( $^8S_{7/2}$ ) ground state of the  $\text{Eu}^{2+}$  ion, to states in the  $4f^65d$  configuration.<sup>15</sup> The high-energy band is a transition from the ground state to the  $e_g$  component of the  $4f^65d$  configuration, while the low-energy band is a transition from the ground state to the  $t_{2g}$  component. The separation between them is due to the 10Dq splitting of the  $5d$  orbitals by the crystal field into two distinct energy levels.

Three qualitatively different spectra have been observed in Eu-doped NaCl depending on the aging of the samples. Figure 1 shows the optical-absorption spectra obtained from samples containing  $\sim 600$  ppm of  $\text{Eu}^{2+}$  for a sample temperature of 25 °C. They correspond to a freshly quenched sample (I), a two-year-old crystal [II(a)], and a six-year-old crystal [II(b)]. The latter two crystals were stored at room temperature and were not subjected to any previous heat treatment since they were grown, two and six years ago, respectively. In all cases, the low-energy band extending from about 320 to 420 nm has a characteristic staircase structure. The high-energy band extending from about 220 to 290 nm presents a well resolved structure in the well aged crystals which is difficult to observe in the optical-absorption spectrum of the same samples after they have been heated at 600 °C for one hour and then quenched to room temperature. The structure of both bands can be more easily observed in the second derivative of the absorption curve which is shown in Fig. 2 for the same three samples from which the spectra presented

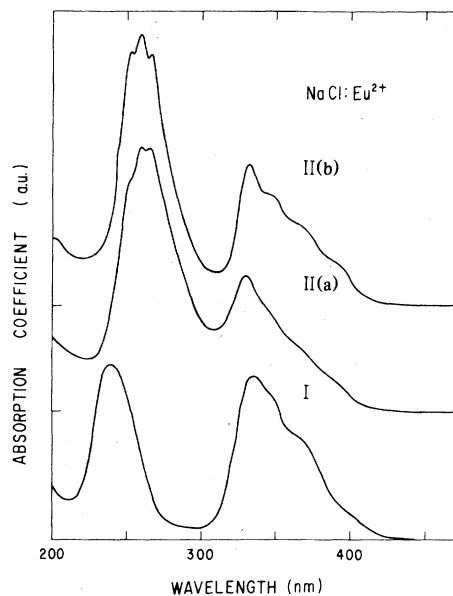


FIG. 1. Room-temperature optical-absorption spectra of  $\text{Eu}^{2+}$  in NaCl with an impurity concentration of 600 ppm for a freshly quenched crystal (I), a two-year-old crystal [II(a)], and a six-year-old crystal [II(b)].

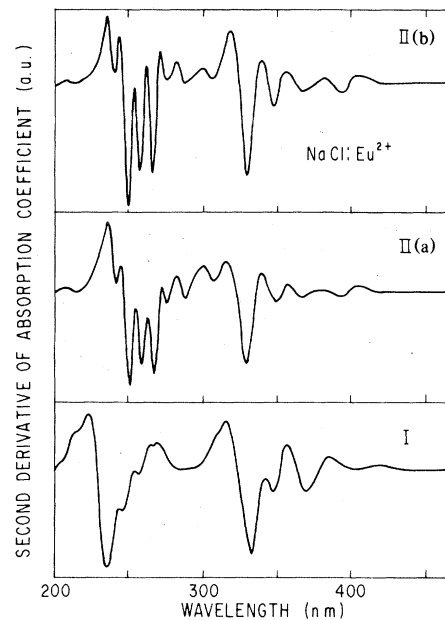


FIG. 2. Second derivative of the optical-absorption spectra shown in Fig. 1 for a sample temperature of 25°C.

TABLE I. Peak position, width, and oscillator strength of the bands composing the broad high- and low-energy bands of spectra I, II(a), and II(b) of  $\text{Eu}^{2+}$  in NaCl at room temperature.

Spectrum	Peak positions (nm)	High-energy band			Center of gravity (nm)	Low-energy band			Center of gravity (nm)
		Bandwidth ( $\text{cm}^{-1}$ )	Oscillator strength ( $10^{-2}$ )			Peak positions (nm)	Bandwidth ( $\text{cm}^{-1}$ )	Oscillator strength ( $10^{-2}$ )	
I	240	5425	4.12	240	400	1545	0.14	347	
					383	1225	0.19		
					370	1255	0.41		
					361	1195	0.27		
					351	1212	0.36		
					342	1620	0.61		
II(a)	262	2237	0.64	262	329	1907	1.15	345	
					393	1168	0.07		
					287	1889	0.70		
					278	1413	0.35		
					382	1152	0.09		
					273	1481	0.53		
II(b)	260	2151	0.75	260	370	1162	0.14	349	
					360	1236	0.18		
					287	1690	0.37		
					279	1213	0.34		
					381	1059	0.13		
					273	1148	0.39		
II(b)	243	2151	0.75	243	361	1145	0.20	349	
					350	1236	0.30		
					266	1296	0.82		
					258	1412	1.02		
					371	1096	0.18		
					250	1328	0.64		
II(b)	243	2151	0.75	243	342	1205	0.21	349	
					330	1412	0.64		
					243	2151	0.75		
					361	1145	0.20		
					258	1412	1.02		
					342	1205	0.21		

TABLE II. Values for the 10Dq splitting of  $\text{Eu}^{2+}$  in several hosts.

Host	Center of gravity of the high-energy band (nm)	Center of gravity of the low-energy band (nm)	10Dq ( $\text{cm}^{-1}$ )	Reference
NaCl (I)	240	347	12 849	This work
NaCl [II(a)]	262	345	9 182	This work
NaCl [II(b)]	260	349	9 809	This work
KCl (I)	243	343	11 997	This work
KCl (II)	244	349	12 331	This work
$\text{EuCl}_2 \cdot \text{H}_2\text{O}$ liquid solution	247	320	9 236	Ganopolskii <i>et al.</i> <sup>a</sup>

<sup>a</sup>Reference 16.

in Fig. 1 were obtained. This presentation allowed us to measure the peak position of the bands composing the broad high- and low-energy bands with great accuracy. The structure on these bands has been interpreted as due to a Coulomb and exchange interaction between the  $5d$  and  $4f$  electrons at about half of the free ion value.<sup>15</sup>

In Table I, the peak position, the width, and the values for the oscillator strength are reported for each of the observed bands in the optical-absorption spectra (I), [II(a)], and [II(b)] of  $\text{Eu}^{2+}$  in NaCl for a sample temperature of 25 °C. In order to calculate values for the oscillator strength, the observed structured bands were decomposed into energy-Gaussian-shape bands following the same procedure as the one described by Hernández *et al.* in a previous paper.<sup>15</sup> With this procedure, values for the oscillator strength were calculated within  $\pm 10\%$ . In Table II values are reported for the measured 10Dq splitting of spectra I, II(a), and II(b) for  $\text{Eu}^{2+}$  in NaCl along with that previously reported by Ganopolskii *et al.*<sup>16</sup> for  $\text{EuCl}_2$  in liquid solutions. This value is very similar to those we have measured for both spectra II(a) and II(b). It is important to notice, that the value for the 10Dq splitting of spectrum II(a) is very similar to that of II(b) and both smaller than that of spectrum I corresponding to the quenched samples. This fact indicates that in the precipitated phases associated with spectra II(a) and II(b), the crystal field at the  $\text{Eu}^{2+}$  site is smaller than at the site occupied by the impurity when it is dispersed in the lattice forming (I–V) dipoles. From now on, we will refer to the NaCl: $\text{Eu}^{2+}$  sample by its characteristic optical-absorption spectrum [I, II(a), and II(b)].

When a well aged crystal is quenched after heating for one hour at 600 °C, spectra II(a) and II(b) are transformed into spectrum I. The integral intensity of the optical-absorption spectrum I is the same, within experimental error, as the one previously measured in II(a) and II(b) before the heat treatment.

This fact indicates that a constant number of  $\text{Eu}^{2+}$  ions is involved and that differences in spectra I and II arise from a change of environment of the impurity ions. After storing the crystals at room temperature for several months, spectrum I faded into II(a), indicating that precipitation has taken place in the crystal matrix.

## 2. KCl samples

The optical-absorption spectrum of the  $\text{Eu}^{2+}$  ion in KCl does not depend as strongly on the aging process of the sample as in the case of NaCl discussed above. Figure 3 shows the observed spectra for an impurity concentration of 270 ppm for: (I) a freshly quenched sample; and (II) a crystal which was stored at room temperature for five years and was not subjected to any heat treatment during this time. By a comparison of spectra I and II, it is evident that the spectrum corresponding to a well aged crystal presents a clearly resolved structure on the high-energy band which is difficult to detect in the spectrum corresponding to the quenched sample. This structure is similar to that observed in spectrum II(a) of  $\text{Eu}^{2+}$  in NaCl. Figure 4 shows the second derivative of the absorption spectra for the same samples. After several months of aging at room temperature, spectrum I transforms into II indicating that precipitation has taken place.

In Table III, the peak position, the width, and the values for the oscillator strength are reported for each of the observed bands in the optical-absorption spectra I and II of  $\text{Eu}^{2+}$  in KCl. As before, in order to obtain values for the oscillator strength, the observed bands were decomposed into energy-Gaussian-shape bands. The 10Dq values corresponding to each spectrum are reported in Table II along with those measured in NaCl for the sake of comparison. It is im-

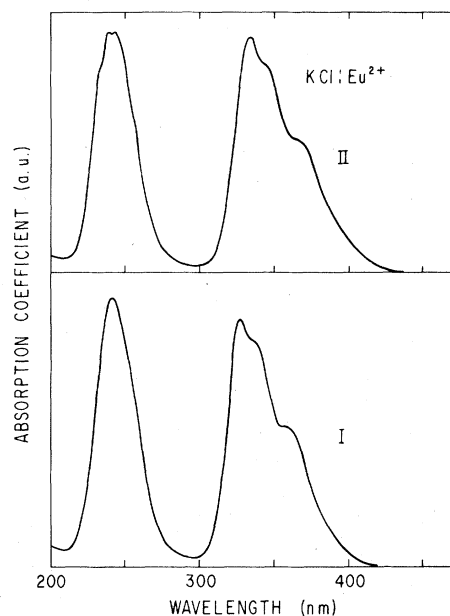


FIG. 3. Room-temperature optical-absorption spectra of  $\text{Eu}^{2+}$  in KCl with an impurity concentration of 270 ppm for a freshly quenched crystal (I) and a five-year-old crystal (II).

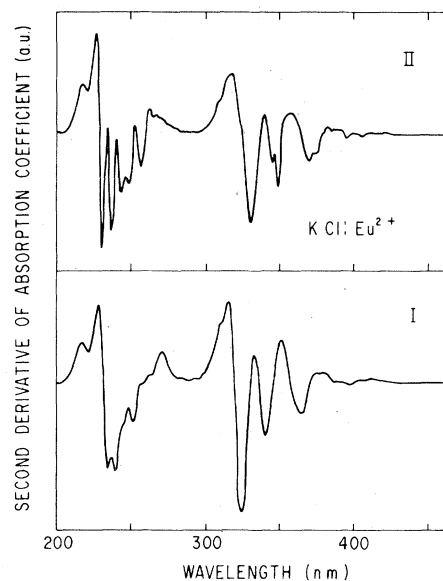


FIG. 4. Second derivative of the optical-absorption spectra shown in Fig. 3 for a sample temperature of 25°C.

TABLE III. Peak position, width, and oscillator strength of the bands composing the broad high- and low-energy bands of spectra I and II of  $\text{Eu}^{2+}$  in KCl at room temperature.

Spectrum	Peak positions (nm)	High-energy band			Center of gravity (nm)	Low-energy band		
		Bandwidth ( $\text{cm}^{-1}$ )	Oscillator strength ( $10^{-2}$ )	Center of gravity (nm)		Peak positions (nm)	Bandwidth ( $\text{cm}^{-1}$ )	Oscillator strength ( $10^{-2}$ )
I	243	5212	3.98	243	393	1661	0.12	343
					379	1430	0.17	
					366	1235	0.33	
					356	1290	0.31	
					344	1423	0.53	
					338	1568	0.37	
					326	1624	1.06	
II	244	1779	0.65	244	398	1695	0.15	349
					267	2190	0.29	
					257	1959	0.63	
					249	1846	0.62	
					244	1779	0.65	
					238	1652	0.59	
					232	2047	0.82	
224	2038	0.23						

portant to notice that the value for the 10Dq splitting of spectrum II is larger than the one of spectrum I. It also indicates that the crystal field at the  $\text{Eu}^{2+}$  site in the precipitated phase of  $\text{Eu}^{2+}$  in KCl, is stronger than at the site occupied by the impurity ion after the sample has been quenched from high temperatures.

## B. Luminescence spectra

### 1. NaCl samples

The emission from the  $\text{Eu}^{2+}$  ion in NaCl can be excited by light lying in the absorption bands. Figure 5 shows the emission spectra, when the excitation is performed at 350 nm, of the same three samples whose optical-absorption spectra are given in Fig. 1. It is clearly apparent from this figure, that the fluorescence spectrum is strongly dependent on the aggregation state of the  $\text{Eu}^{2+}$  ions and consists of four bands peaking at 410, 427, 439, and 485 nm. The decomposition of the emission spectra for samples I, II(a), and II(b) is shown in the same figure. The emission band peaking at 427 nm is the most prominent in the quenched samples (I), although a very small component at 485 nm is also observed in crystals with an impurity concentration of  $\sim 600$  ppm or greater. However, it should be pointed out that the intensity of this later emission is strongly dependent on the speed of the quenching and it is not observed in quenched samples with a lower europium concentration (100 ppm). The presence of the 485-nm emission band in the heavily doped crystals immediately after quenching is taken to mean that the quenching is not rapid enough to prevent some aggregation occurring before the sample reaches room temperature. On the other hand, the emission bands peaking at 439 and 485 nm are the most dominant in the well aged crystals [II(a) and II(b)], while

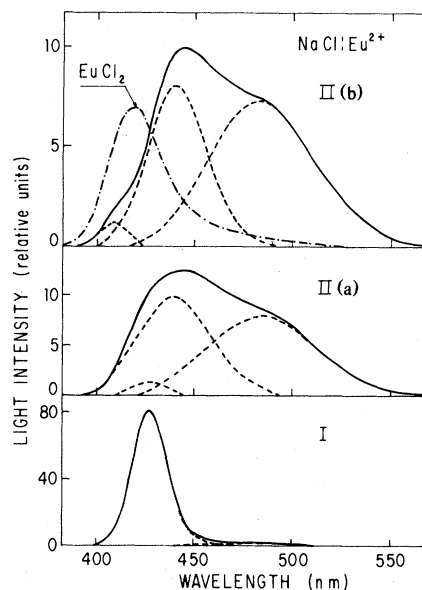


FIG. 5. Emission spectra of  $\text{Eu}^{2+}$  in NaCl (600 ppm), excited at 350 nm of the same three samples whose optical-absorption spectra are shown in Fig. 1. The decomposition of the spectra into the bands at 410, 427, 439, and 485 nm is shown by the dashed lines. The chain curve stands for the emission of powdered  $\text{EuCl}_2$ , also excited at 350 nm.

that peaking at 410 nm appears only in the oldest one [II(b)]. However, this later band can be produced in the crystals previously quenched by: (1) annealing the samples at 500 °C for 24 h and then decreasing the temperature of the furnace at a rate of 15 °C/h; and (2) annealing the samples at 300 °C for about 70 h. The emission spectrum of powdered  $\text{EuCl}_2$ , when the excitation is performed at 350 nm, is also presented in Fig. 5 for the sake of comparison. In Table IV, the peak position and the width are given

TABLE IV. Peak position and width of the emission bands of  $\text{NaCl}:\text{Eu}^{2+}$ ,  $\text{KCl}:\text{Eu}^{2+}$ , and powdered  $\text{EuCl}_2$  at 25 °C.

Host	Position (nm)	Width (eV)
NaCl	410	0.13
	427	0.14
	439	0.22
	485	0.30
KCl	419	0.15
	427	0.17
$\text{EuCl}_2$	417	0.23

for all the emission bands of  $\text{Eu}^{2+}$  in NaCl for a sample temperature of 25 °C.

The excitation spectrum for each emission band has been obtained at room temperature in the scan range 220–500 nm. Figure 6 shows the excitation spectra for the 427-nm band of quenched samples of NaCl:Eu<sup>2+</sup> for two different concentrations (100 and 600 ppm). Although there exist some minor differences between the two spectra, the two broad-band structure referred to earlier is clearly seen. The relative intensities of the high- and low-energy bands in the excitation spectrum are not comparable with those of the optical-absorption spectrum since the former was not corrected for intensity changes with wavelength of the excitation lamp. The presence of the  $e_g$  band in the excitation spectrum indicates a decay from the  $e_g$  level to the  $t_{2g}$ , from which the fluorescence originates.

The excitation spectra for the emission bands peaking at 410, 439, and 485 nm in the well aged samples of NaCl:Eu<sup>2+</sup> are presented in Fig. 7. The excitation spectra for the emissions at 410 and 485 nm are very similar to the absorption spectrum, while the emission at 439 nm is, in addition, strongly excited by light lying between the two absorption bands (292 and 322 nm). The values for the 10Dq splitting measured from the excitation spectra agree quite well with those measured from the optical-absorption spectra. It must be pointed out, that the peak position of the emission bands is the same in spite of the excitation wavelength in the high- as well as in the low-energy band.

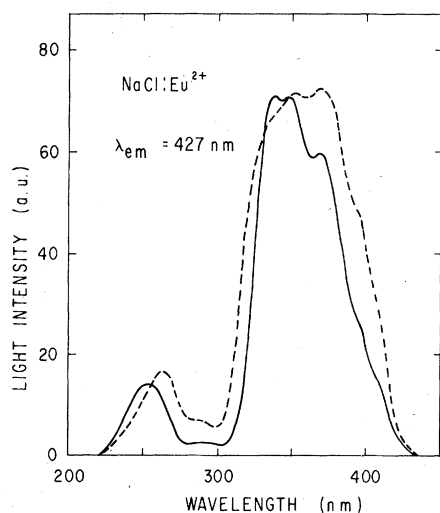


FIG. 6. Excitation spectra for the emission band peaking at 427 nm of quenched samples of NaCl:Eu<sup>2+</sup> for two different concentrations; continuous line: 100 ppm; dashed line: 600 ppm.

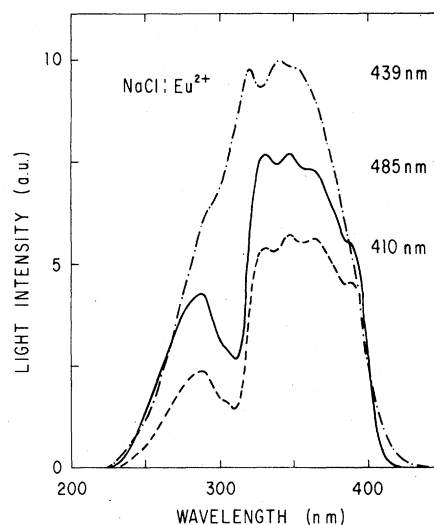


FIG. 7. Excitation spectrum for the emission bands peaking at 410, 439, and 485 nm in the well aged crystals of NaCl doped with 600 ppm of divalent europium.

## 2. KCl samples

Figure 8 shows the observed emission spectra at room temperature for Eu<sup>2+</sup> in KCl single crystals when the excitation is performed at 350 nm. As in the case of NaCl discussed above different emission spectra were observed in quenched (I) and well aged crystals (II). The quenched samples only exhibit an

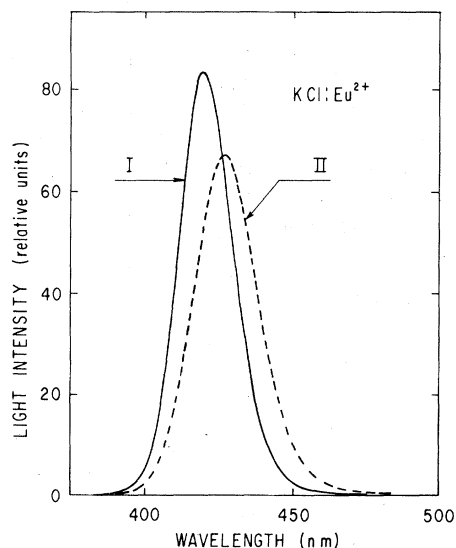


FIG. 8. Emission spectra of Eu<sup>2+</sup> in KCl for the same two samples whose optical-absorption spectra are shown in Fig. 3, when the excitation is performed at 350 nm.

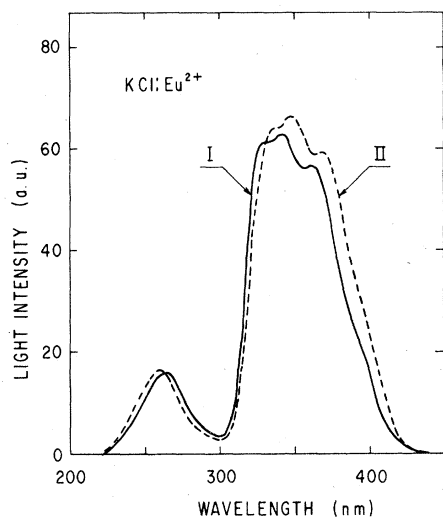


FIG. 9. Excitation spectrum of  $\text{Eu}^{2+}$  in KCl for the two emission bands peaking at 419 and 427 nm.

emission band peaking at 419 nm. However, in contrast with the well aged samples of NaCl, only one emission band peaking at 427 nm was observed in crystals of KCl (270 ppm) which were stored at room temperature for five years without being subjected to any previous heat treatment. In Table IV, the peak position and width for the observed emission bands of  $\text{Eu}^{2+}$  in KCl are reported along with those of NaCl for the sake of comparison.

In Fig. 9 the excitation spectra for the two emission bands peaking at 419 and 427 nm are given. They correlate quite well with the optical-absorption spectra (I) and (II) previously shown in Fig. 3, and clearly show that the  $10Dq$  splitting of the excitation spectrum corresponding to the well aged samples is larger than that of the quenched ones. As in the case of NaCl, the presence of the  $e_g$  level in the excitation spectrum indicates a decay from the  $e_g$  level to the  $t_{2g}$ , from which the fluorescence originates. In this case, the peak position of the emission bands is also the same in spite of the excitation wavelength in the high- as well as in the low-energy band.

### C. Annealing experiments

#### 1. NaCl samples.

The evolution of the emission bands as a function of the temperature for a two-year-old sample (100 ppm) of  $\text{NaCl}:\text{Eu}^{2+}$  has been determined in the range 25–600°C. The emission spectrum of this sample consists initially of the 427-, 439-, and 485-nm bands and the corresponding optical-absorption spectrum is similar to that of the quenched one, although the peak position of the high-energy band is displaced to

longer wavelengths (243 nm) and the  $10Dq$  value is smaller ( $12499\text{ cm}^{-1}$ ) indicating that precipitation has taken place. With increasing temperature several changes occur in the emission spectrum. The emission band peaking at 485 nm wholly disappears at about 250°C, while the 439-nm band does near 400°C. At the same time the emission band at 427 nm is enhanced. The intensities of these different emission bands as a function of the temperature are collected in Fig. 10. To make these measurements, the sample was heated for 30 min at the temperatures shown in the figure and then quenched to room temperature to record the emission spectrum. The same type of results as those mentioned above were obtained in the oldest sample II(b) (600 ppm) although it was found in addition that the emission band at 410 nm disappears at about 430°C, also enhancing the emission at 427 nm. These results indicate that the emission bands at 410, 439, and 485 nm are due to different types of precipitates of  $\text{Eu}^{2+}$  in the NaCl host, which dissolve when the temperature increases. They also indicate that the precipitated phase responsible for the emission band at 485 nm is stable at lower temperatures than those responsible for the emission bands peaking at 410 and 439 nm. On the other hand, during the dissolution of the precipitated phases, the main change in the optical-absorption spectrum is that the high-energy band moves from 260 to 240 nm increasing the value of the  $10Dq$  splitting.

The aging of quenched samples (600 ppm) has also been studied at five different annealing temperatures: 25, 50, 100, 200, and 300°C. As an example, Fig. 11 shows the evolution of the emission spectrum as a function of the aging time at 50 and 100°C. In Fig. 12, the quantitative results of this evolution are presented for 25 and 100°C. The aging at room temperature (25°C) produces only the 485-nm band for times up to ~350 h. However, annealing the samples at 100°C induces the growth of the emission bands at 485 and 439 nm up to ~20 h. As the an-

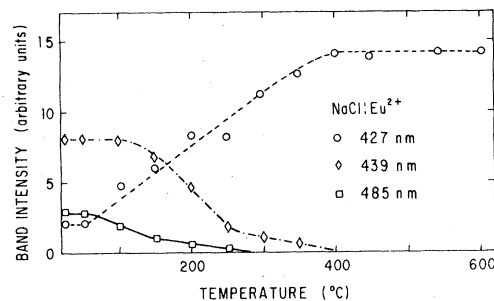


FIG. 10. Evolution of the intensity (area under the curve) of the emissions bands at 427, 439, and 485 nm of  $\text{Eu}^{2+}$  in NaCl (100 ppm) as a function of the annealing temperature.



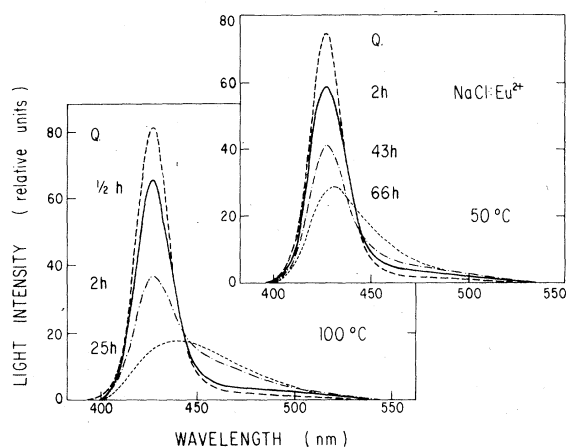


FIG. 11. Evolution of the emission spectrum, excited at 350 nm, for  $\text{Eu}^{2+}$  in NaCl (600 ppm) as a function of the aging time for quenched samples kept at 50 and 100°C.

nealing treatment proceeds a saturation of the growth of the 485-nm band takes place and the 439-nm band continues to grow. The same type of behavior is observed at 50 and 200°C, although the evolution is slower at the former temperature and faster at the latter. Annealing the samples at 300°C produces the 439- and the 410-nm bands in about 10 and 70 h, respectively. At this point it is important to mention, that in the heavily doped samples ( $\sim 2000$  ppm), the aging at room temperature produces the growth of the 485- and 439-nm bands in 5 and 150 h, respec-

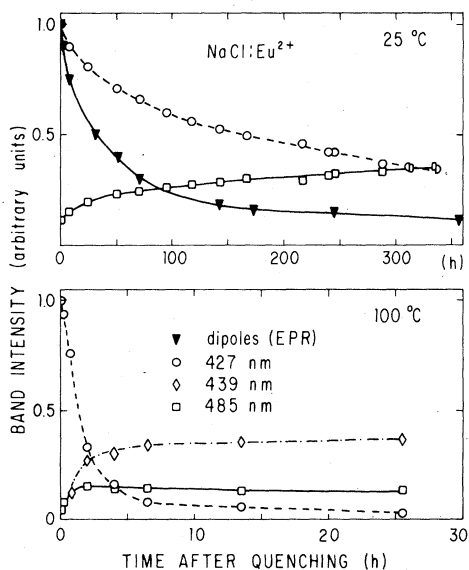


FIG. 12. Intensity (area under the curve) of the emission bands of  $\text{Eu}^{2+}$  in NaCl (600 ppm) vs the aging time at 25 and 100°C. The dipole decay at room temperature is also shown.

tively. Also, the same behavior of the emission bands, at the different annealing temperatures as the one reported above for samples doped with 600 ppm, is observed in the heavily doped samples, although the time involved is quite smaller.

The decay of  $\text{Eu}^{2+}$ -cation vacancy dipoles (I-V) at room temperature as a function of the elapsed time after a fast quenching from 600°C was measured by EPR and the result is also plotted in Fig. 12 for the sake of comparison. To do these measurements, the same procedure as the one we have described in a previous paper<sup>11</sup> was employed. From the data given in this figure, it is clearly evident that the intensity of the emission band at 427 nm decays at room temperature more slowly than the EPR signal intensity due to (I-V) dipoles. Therefore, the intensity of this band is not proportional to the concentration of free  $\text{Eu}^{2+}$ -cation vacancy pairs.

## 2. KCl samples

The emission spectrum of the well aged samples (270 ppm) of  $\text{Eu}^{2+}$  in KCl only shows one band peaking at 427 nm. On increasing the temperature, no variation is observed in its intensity, as well as in the width for temperatures up to 80°C. In the range 90–150°C the maximum of the emission band moves to shorter wavelengths, i.e., from 427 to 419 nm. This apparent displacement of the maximum of the emission band is due to a decrease of the intensity of the 427-nm band on the benefit of that peaking at 419 nm. This fact can be appreciated by decomposing the observed emission spectrum into both bands. Figure 13 shows the emission spectra at four different temperatures, as well as the decomposition which was performed into the 427- and 419-nm bands in each case. In Fig. 14, the quantitative evolution of the intensities of these two bands as a function of temperature is presented. Reference to this figure shows that the thermal resolution of the precipitated phase of divalent europium in the potassium chloride host takes place in a narrow range of temperatures (90–150°C). In order to make these measurements, the same procedure as the one described previously for the NaCl crystal was employed. During the dissolution of the precipitated phase, the changes in the optical-absorption spectrum are only minor compared with those that occur in NaCl, being the most significant the decrease of the  $10Dq$  value.

When a sample which has been quenched from 600°C is stored at room temperature, the intensity and the width of the emission band at 419 nm do not change, within the experimental error, for times up to  $\sim 1000$  h. Also, no change was observed in the optical-absorption spectrum. However, the EPR signal intensity due to (I-V) dipoles decreased about 10% of its original value in this time. This result in-

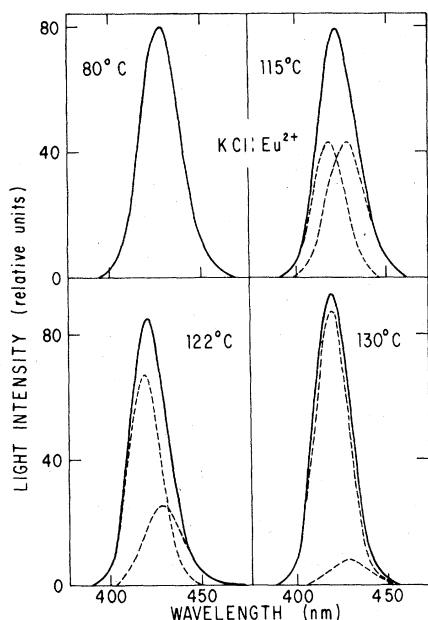


FIG. 13. Emission spectra of  $\text{Eu}^{2+}$  in KCl at four different temperatures in the resolution process of well aged samples (270 ppm). The decomposition into 419- and 427-nm bands is given by the dashed curves.

icates, therefore, that the intensity of the emission band at 419 nm is not proportional to the concentration of isolated dipoles. Aging the samples at  $50^\circ\text{C}$  produces the appearance of the emission band at 427 nm in  $\sim 20$  h, indicating that precipitation is taking place. The intensities of the 427- and 419-nm bands as a function of time for an aging temperature of  $50^\circ\text{C}$  are presented in Fig. 15, from which one can observe that the emission band at 419 nm in the quenched samples is transformed  $\sim 85\%$  into the 427-nm band in about 700 h.

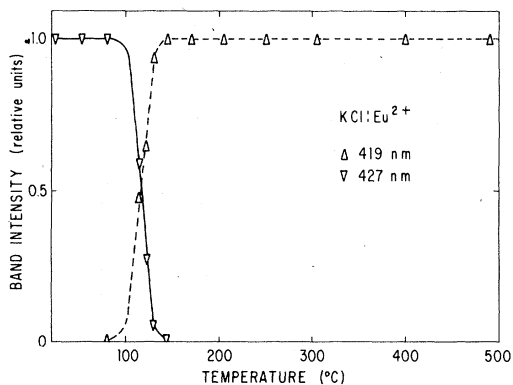


FIG. 14. Evolution of the intensity of the emission bands of  $\text{Eu}^{2+}$  in KCl (270 ppm) at 419 and 427 nm as a function of the annealing temperature.

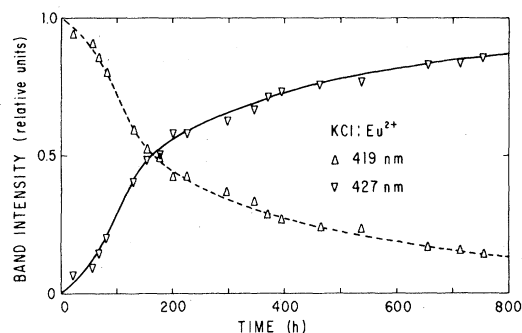


FIG. 15. Intensity of the emission bands of  $\text{Eu}^{2+}$  in KCl (270 ppm) at 419 and 427 nm vs the aging time at  $50^\circ\text{C}$ .

#### IV. DISCUSSION

The samples employed in this work have been stored a long time at room temperature and therefore most of the impurity will be found forming a segregated phase. The most significant features to infer from the results given above for NaCl doped with  $\text{Eu}^{2+}$  are: (1) the occurrence of three emission bands peaking at 410, 439, and 485 nm in our well aged samples (600 ppm); (2) their different thermal stabilities; (3) the decrease of the intensities of all of these bands on increasing the temperature on the benefit of the emission band at 427 nm, which is also the one observed after quenching; and (4) the growth of these bands as a function of time at different aging temperatures in the previously quenched samples.

The emission band peaking at 427 nm in the quenched samples can be ascribed, in principle, to isolated  $\text{Eu}^{2+}$ -cation vacancy dipoles. However, taking Fig. 12 as a reference, it is evident that the dipole decay at room temperature is faster than the decay of the intensity of this band, which is therefore not proportional to the concentration of isolated dipoles. From this fact, it is possible to conclude that the first products of aggregation (dimers, trimers, etc.) also emit at the same energy, or slightly shifted, to that of the isolated dipoles. This conclusion is similar to that reported by Pascual *et al.*<sup>17</sup> for  $\text{Pb}^{2+}$  in NaCl, for which the emission band observed in the quenched samples was ascribed not only to isolated dipoles but also to some other initial products of aggregation.

The correlation between the emission band peaking at 410 nm in the well aged samples and the emission spectrum of  $\text{EuCl}_2$  is quite satisfactory. This agreement indicates that the precipitated phase responsible for the emission band at 410 nm in crystals stored at room temperature for six years is the stable dihalide phase  $\text{EuCl}_2$ . This assignment is in agreement with our previous investigation,<sup>11</sup> in which  $\text{EuCl}_2$  was detected by x-ray diffraction analysis in the same

crystals as those used in this work, and with the fact that the value for the 10Dq splitting measured in spectrum II(b) is very similar to that reported by Ganopolskii *et al.*<sup>16</sup> for  $\text{EuCl}_2$  in liquid solutions.

The behavior reported above for the emission bands at 439 and 485 nm under dissolution and aging processes is very similar to that previously reported by Suzuki for the metastable plate zones of  $\text{Ca}^{2+}$  ions in NaCl. Therefore, we have ascribed the emissions at 439 and 485 nm of  $\text{Eu}^{2+}$  in NaCl to the metastable  $\text{EuCl}_2$ -like plate zones parallel to  $\{111\}$  and  $\{310\}$  planes of the matrix lattice, respectively. Evidence supporting these assignments is given by the following facts: (1) electron microscopy measurements performed by Yacamán and Basset<sup>18</sup> in the same samples as those employed in this work, revealed decoration patterns similar to those found by Suzuki for the metastable  $\text{CaCl}_2$ -like plate zones of calcium ions in NaCl; (2) in those crystals for which the 439- or the 485-nm band is the most prominent, we found an optical-absorption spectrum with a 10Dq value very similar to that of spectrum II(b). This fact indicates that the crystal field at the  $\text{Eu}^{2+}$  site in the precipitated phases responsible for the emissions at 439 and 485 nm is very similar to that at the site occupied by this ion in the  $\text{EuCl}_2$  matrix; (3) the excitation spectrum obtained by monitoring the fluorescence at 439 and 485 nm is very similar to that obtained from the emission at 410 nm, indicating that the precipitated phases responsible for these three emissions are very similar; and (4) the  $\{310\}$  plate zone is thermally less stable than the  $\{111\}$  and grows first during the aging process at low temperatures. This behavior is the same as the one found for the precipitated phases associated with the emissions at 485 and 439 nm, respectively.

The presence of the stable dihalide phase  $\text{EuCl}_2$  in  $\text{Eu}^{2+}$ -doped NaCl reported above is in agreement with our previous investigation.<sup>11</sup> However, at variance with that work evidence of two additional precipitated phases has been given in the present investigation thanks to the high resolution associated with the luminescence technique which appears to be a powerful tool for the investigation of precipitation phenomena.

On the other hand, the most interesting results obtained in the  $\text{KCl}:\text{Eu}^{2+}$  samples are: (1) the occurrence of only one emission band peaking at 427 nm in the well aged samples; and (2) the thermal resolution of the precipitated phase in a narrow range of temperatures, which results in the growth of an emission band at 419 nm. This later band is the same as the one observed in the well aged samples after a fast quenching. As in the case of NaCl discussed above, the emission at 419 nm in the quenched samples is ascribed not only to isolated  $\text{Eu}^{2+}$ -cation vacancy dipoles but also to the initial products of aggregation. The emission band at 427 nm

in the well aged samples has been tentatively ascribed to the so-called Suzuki phase of divalent europium in the potassium chloride host with the stoichiometry  $6\text{KCl}\cdot\text{EuCl}_2$ . Evidence in favor of this assignment can be stated as follows: (1) The thermal resolution of the precipitated phase occurs in a narrow range of temperatures, which is a result similar to that previously reported for the dissolution of the Suzuki phase of  $\text{Cd}^{2+}$  and  $\text{Sr}^{2+}$  in NaCl.<sup>19,20</sup> Also the range of temperatures is similar for these systems, and (2) the value for the 10Dq splitting measured in both the optical and excitation spectra of these well aged crystals is larger than the one measured in the spectrum corresponding to the quenched ones. This result indicates that the crystal field at the  $\text{Eu}^{2+}$  site in the precipitated phase may be larger than at the site occupied by the divalent impurity ion after the same samples have been quenched. This situation is expected for the precipitated Suzuki phase. In fact, theoretical calculations performed in the systems  $\text{NaCl}\cdot\text{MnCl}_2$  and  $\text{NaCl}\cdot\text{CdCl}_2$  have shown,<sup>21-23</sup> that in the Suzuki phase, the nearest-neighbor chlorine ions of the divalent ion are at smaller distance than when the impurity is dispersed in the lattice forming (I-V) dipoles, therefore increasing the crystal field at the site occupied by the divalent impurity in the precipitated phase.

Finally, we would like to comment that the behavior of the  $\text{Eu}^{2+}$  ion in NaCl reported in this work is very similar to that of  $\text{Pb}^{2+}$ -doping NaCl in the following points: (1) in both cases, the optical absorption and emission spectra are quite sensitive to the state of aggregation of the impurity ions, and (2) it is known<sup>11,17</sup> that both  $\text{Eu}^{2+}$  and  $\text{Pb}^{2+}$  segregate in the NaCl matrix to form the stable dihalide phase  $M\text{Cl}_2$  ( $M = \text{Pb}, \text{Eu}$ ). On the other hand, the systems  $\text{KCl}\cdot\text{EuCl}_2$  and  $\text{KCl}\cdot\text{PbCl}_2$  are similar in the sense that, in both cases, the optical absorption and emission spectra are less sensitive to the aggregation state of the impurity ions than for NaCl. For  $\text{Pb}^{2+}$ -doped KCl, evidence indicating that Suzuki-phase precipitates can be formed has been recently gathered.<sup>24,25</sup> The similarities between these two systems may support our assignment that the precipitated phase of divalent europium ions in the potassium chloride host is the Suzuki phase. Evidence, obtained through x-ray or electron-microscopy measurements is, however, required in order to firmly establish this assignment.

#### ACKNOWLEDGMENTS

We thank W. K. Cory for growing the crystals and Professor O. Cano and Fís. A. Cordero-Borboa for taking some of the measurements. This work was carried out while one of us (F.J.L.) was on leave at the University of México, and he wishes to thank Dr. Flores Valdés for his hospitality.

- \*Permanent address: Departamento de Optica y Estructura de la Materia, Universidad Autónoma de Madrid, Madrid-34, Spain.
- <sup>1</sup>S. Miyake and K. Suzuki, *J. Phys. Soc. Jpn.* **2**, 702 (1954).  
<sup>2</sup>S. Miyake and K. Suzuki, *Acta Crystallogr.* **7**, 514 (1954).  
<sup>3</sup>K. Suzuki, *J. Phys. Soc. Jpn.* **10**, 794 (1955).  
<sup>4</sup>K. Suzuki, *J. Phys. Soc. Jpn.* **13**, 179 (1958).  
<sup>5</sup>K. Suzuki, *J. Phys. Soc. Jpn.* **16**, 67 (1961).  
<sup>6</sup>Y. Yal-Jamal (unpublished), quoted by A. I. Sors and E. Lilley, *Phys. Status Solidi A* **27**, 469 (1975).  
<sup>7</sup>G. A. Andreev, M. Hartmanová, and V. A. Klimov, *Phys. Status Solidi A* **41**, 679 (1977).  
<sup>8</sup>M. J. Yacamán and R. W. Vook, in *Proceedings of the 35th Annual Meeting of the Electron Microscopy Society of America, Boston, 1976*, edited by G. W. Bailey (Claitor, Baton Rouge, 1977), p. 258.  
<sup>9</sup>J. A. Chapman and E. Lilley, *J. Mater. Sci.* **10**, 1154 (1975); D. L. Kirk, A. R. Kahn, and P. L. Pratt, *J. Phys. D* **8**, 2013 (1975).  
<sup>10</sup>A. I. Sors and E. Lilley, *Phys. Status Solidi A* **32**, 533 (1975).  
<sup>11</sup>J. García M., J. Hernández A., E. Carrillo H., and J. Rubio O., *Phys. Rev. B* **21**, 5012 (1980).  
<sup>12</sup>G. Vlasák and M. Hartmanová, *Krist. Tech.* **10**, 369 (1955).  
<sup>13</sup>R. A. Cooley and D. M. Yost, *Inorg. Synth.* **2**, 71 (1946).  
<sup>14</sup>J. Hernández A., W. K. Cory, and J. Rubio O., *Jpn. J. Appl. Phys.* **18**, 533 (1979).  
<sup>15</sup>J. Hernández A., W. K. Cory, and J. Rubio O., *J. Chem. Phys.* **72**, 198 (1980).  
<sup>16</sup>V. I. Ganopolskii, V. F. Barkovskii, and N. P. Ipatova, *Zh. Prikl. Spektrosk.* **5**, 805 (1966).  
<sup>17</sup>J. L. Pascual, L. Arizmendi, F. Jaque, and F. Agulló-López, *J. Lumin.* **17**, 325 (1978).  
<sup>18</sup>M. José Yacamán and G. A. Bassett, *J. Appl. Phys.* **47**, 2313 (1976).  
<sup>19</sup>M. Hartmanová, I. Thurzo, and S. Besedicová, *J. Phys. Chem. Solids* **38**, 587 (1977).  
<sup>20</sup>R. Capelletti and E. Okuno, *J. Electrochem. Soc.* **120**, 565 (1973).  
<sup>21</sup>A. I. Sors and E. Lilley, *Phys. Status Solidi A* **27**, 469 (1975).  
<sup>22</sup>F. Bassani and F. G. Fumi, *Nuovo Cimento* **11**, 274 (1954).  
<sup>23</sup>U. Oseguera V., H. Murrieta S., C. Ruíz-Mejía, and J. Rubio O., *J. Chem. Phys.* **73**, 1132 (1980).  
<sup>24</sup>P. G. Bertoldi, R. Capelletti, and F. Fermi, in *Proceedings of the 3rd Europhysics Conference on Lattice Defects in Ionic Crystals*, University of Kent at Canterbury, U.K., Sept. 17–21, 1979, edited by J. H. Strange (unpublished), p. A48.  
<sup>25</sup>M. Locatelli, E. Zecchi, and R. Capelletti, in *Proceedings of the 3rd Europhysics Conference on Lattice Defects in Ionic Crystals*, University of Kent at Canterbury, U.K., Sept. 17–21, 1979, edited by J. H. Strange (unpublished), p. A48.